JACC: BASIC TO TRANSLATIONAL SCIENCE VOL. 9, NO. 4, 2024

ORIGINAL RESEARCH - PRECLINICAL

Carotid Baroreceptor Stimulation Improves Pulmonary Arterial Remodeling and Right Ventricular Dysfunction in Pulmonary Arterial Hypertension

Jing Wang, MM,[a,b,c,d,*] Jie Chen, MM,[a,b,c,e,*] Ling Shu, MM,[a,b,c] Ruoliu Zhang, MB,[a,b,c] Mingyan Dai, MD,[a,b,c] Xuesheng Fang, MB,[a,b,c] Zhiling Hu, MB,[a,b,c] Lingling Xiao, MB,[a,b,c] Zhaoqing Xi, MB,[a,b,c] Junxia Zhang, MD,[f] Mingwei Bao, MD[a,b,c]

VISUAL ABSTRACT

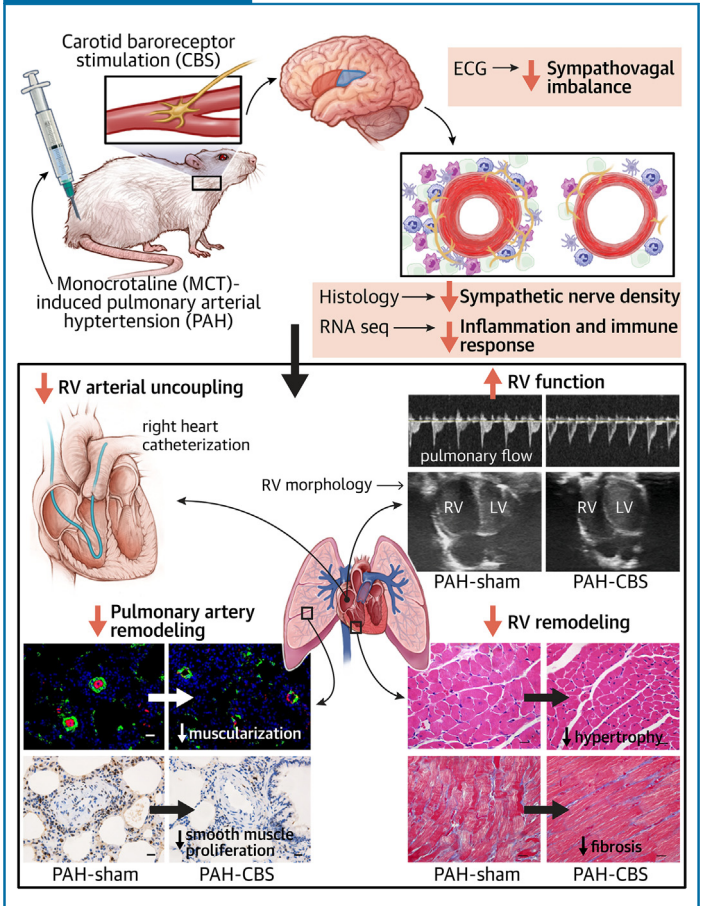

Wang J, et al. J Am Coll Cardiol Basic Trans Science. 2024;9(4):475-492.

HIGHLIGHTS

- **Autonomic nervous system imbalance is intricately associated with the severity and prognosis of PAH.**
- **CBS is a non-pharmaceutical intervention for autonomic neuromodulation.**
- **CBS ameliorated pulmonary arterial remodeling and RV dysfunction in MCT-induced PAH rats.**
- **The protective effects of CBS on PAH may be mediated through the inhibition of sympathetic overactivation and inflammatory immune responses.**

ISSN 2452-302X https://doi.org/10.1016/j.jacbts.2024.01.012

JACC: BASIC TO TRANSLATIONAL SCIENCE VOL. 9, NO. 4, 2024
APRIL 2024:475–492

ABBREVIATIONS AND ACRONYMS

CBS = carotid baroreceptor stimulation

Ea = arterial elastance

Eed = end-diastolic elastance

Ees = end-systolic elastance

HF = high-frequency

LF = low-frequency

MCT = monocrotaline

PA = pulmonary artery

PAH = pulmonary arterial hypertension

PAP = pulmonary artery pressure

RV = right ventricle/ventricular

TH = tyrosine hydroxylase

SUMMARY

Autonomic nervous system imbalance is intricately associated with the severity and prognosis of pulmonary arterial hypertension (PAH). Carotid baroreceptor stimulation (CBS) is a nonpharmaceutical intervention for autonomic neuromodulation. The effects of CBS on monocrotaline-induced PAH were investigated in this study, and its underlying mechanisms were elucidated. The results indicated that CBS improved pulmonary hemodynamic status and alleviated right ventricular dysfunction, improving pulmonary arterial remodeling and right ventricular remodeling, thus enhancing the survival rate of monocrotaline-induced PAH rats. The beneficial effects of CBS treatment on PAH might be mediated through the inhibition of sympathetic overactivation and inflammatory immune signaling pathways. (J Am Coll Cardiol Basic Trans Science 2024;9:475–492)

Pulmonary arterial hypertension (PAH) is characterized by endothelial dysfunction and abnormal vascular remodeling, leading to right heart failure and even death.[1] PAH is likely to result from multiple mechanisms, including a cancer-like metabolic phenotype, mutation of the bone morphogenetic protein type II receptor, altered immunity, increased inflammation, and excessive activation of the neuroendocrine system. The main pathologic features of PAH consist of endothelial dysfunction, proliferation of vascular smooth muscle cells, progressive arterial wall hypertrophy, and subtotal luminal obliteration.[2] In the past 2 decades, various vasodilators have been developed for the treatment of patients with PAH, including prostaglandins, phosphodiesterase-5 inhibitors, endothelin receptor antagonists, and soluble guanylate cyclase stimulators. However, the prognosis for patients with PAH remains poor. The results of the REVEAL (Registry to Evaluate Early and Long-Term PAH Disease Management) registry showed that the 1-year survival rate for patients with newly diagnosed PAH was only 86%, and the 5-year survival rate was only 61%.[3]

Increased sympathetic nervous activity,[4] decreased parasympathetic nervous activity, and depressed baroreflex sensitivity[5] have been confirmed in patients with PAH, which were associated with the severity and poor prognosis of patients with PAH. The adventitia of the pulmonary artery (PA) is innervated by abundant sympathetic and parasympathetic nerves.[6] Neurotransmitters secreted by adrenergic nerve fibers modulate pulmonary vascular function.[6] Increased pulmonary vascular resistance is mediated by α-adrenoreceptors upon sympathetic nerve stimulation.[7] Nowadays, multiple lines of study focused on the role of neurohormonal activation in the pathogenesis of PAH. The rebalancing of the autonomic nervous system is considered a potential therapeutic strategy for PAH.[8]

Previous studies have reported that adrenergic receptor blockers improved pulmonary arterial remodeling and right ventricular (RV) dysfunction in experimental rat models with PAH.[9-11] However, several clinical trials have indicated that β-blockers have adverse side effects on exercise capacity and hemodynamic status in patients with PAH.[12,13] Hence, the use of β-blockers is greatly limited in the management of PAH. In recent years, novel nonpharmacologic strategies of autonomic neuromodulation, including transection of the cervical sympathetic trunk,[14] electric vagal nerve stimulation,[15] renal denervation,[16] and PA denervation,[17] have been found to exert potential therapeutic effects on PAH in animal models. Additionally, several clinical trials have shown that PA denervation

From the [a]Department of Cardiology, Renmin Hospital of Wuhan University, Wuhan, China; [b]Cardiovascular Research Institute, Wuhan University, Wuhan, China; [c]Hubei Key Laboratory of Cardiology, Wuhan, China; [d]State Key Laboratory of Cardiovascular Disease, Heart Failure Center, National Center for Cardiovascular Diseases, Fuwai Hospital, Chinese Academy of Medical Sciences and Peking Union Medical College, Beijing, China; [e]Japan Friendship Hospital (Institute of Clinical Medical Sciences), Chinese Academy of Medical Sciences & Peking Union Medical College, Beijing, China; and the [f]Department of Endocrinology, Taikang Tongji (Wuhan) Hospital, Wuhan, China. *Drs Wang and Chen contributed equally to this work.
The authors attest they are in compliance with human studies committees and animal welfare regulations of the authors' institutions and Food and Drug Administration guidelines, including patient consent where appropriate. For more information, visit the Author Center.

Manuscript received October 4, 2023; revised manuscript received January 2, 2024, accepted January 3, 2024.

significantly improves 6-minute walk distance and reduces pulmonary vascular resistance in patients with several types of pulmonary hypertension.[18,19]

Carotid baroreceptor stimulation (CBS) could rebalance autonomic nervous system by stabilizing sympathetic nerve activity and enhancing vagal nerve activity. Several studies have demonstrated that CBS protected against refractory hypertension and heart failure in humans.[20,21] Excitingly, our previous work has shown that CBS reduces blood pressure in rats with obesity-related hypertension.[22] We also found that CBS could improve cardiac dysfunction and left ventricular remodeling in canines with chronic heart failure.[23] The imbalance of the autonomic nervous system is closely related to the severity and prognosis of patients with PAH, but its specific mechanisms involved in the development of PAH remain unclear. Thus, the aim of this study was to characterize the role of CBS in PAH. We hypothesized that CBS delays PAH progression, improves pulmonary arterial remodeling, and alleviates RV dysfunction by rebalancing autonomic nervous system in rats with monocrotaline (MCT)-induced PAH.

METHODS

ANIMALS AND STUDY PROTOCOL. Male Sprague-Dawley rats (6-8 weeks old, 180-220 g) were obtained from Hunan SJA Laboratory Animal. The experimental protocol was approved by the institutional animal care and use committee at the Renmin Hospital of Wuhan University (WDRM 20210810) and followed the National Institutes of Health Guide for the Care and Use of Laboratory Animals. The rats were housed at a temperature of 20 to 25 °C and a humidity level of 70% under a 12-hour light/dark cycle with ad libitum feeding.

In the pathophysiological study, 32 Sprague-Dawley rats were randomly divided into 4 groups: con-sham (n = 7), con-CBS (n = 7), PAH-sham (n = 9), and PAH-CBS (n = 9). After adaptive feeding for 1 week, some rats were implanted with the CBS device, whereas others were implanted with a CBS model as controls. One week after surgery, some rats with the CBS device (PAH-CBS group) and the CBS model (PAH-sham group) were given a single intraperitoneal injection of MCT 60 mg/kg to induce PAH. The control animals (con-CBS and con-sham group) were injected with an equal dose of normal saline instead. Simultaneously, the CBS device was switched on and stimulus signals were emitted for 4 weeks until the end of the experiment. At the fourth week, echocardiography, noninvasive blood pressure measurement, heart rate variability, pulmonary arterial pressure (PAP), and the RV pressure-volume loop were measured. Arterial and venous blood samples were obtained for arterial blood gas analysis and hepatorenal function detection. Then, the rats were sacrificed and the tissue samples were collected for further measurement (**Figure 1**).

Additionally, another 20 Sprague-Dawley rats were used to examine the effects of CBS on survival rate of rats with PAH. The rats were randomly divided into PAH-sham (n = 10) and PAH-CBS (n = 10) groups. After adaptive feeding for 1 week, the rats underwent implantation with either a CBS device or a CBS model. One week after surgery, both the rats with the CBS device (PAH-CBS group) and those with a CBS model (PAH-sham group) were given a single intraperitoneal injection of MCT 60 mg/kg to induce PAH. At the same time, the CBS device was switched on, and stimulus signals were emitted for 10 weeks until the end of the experiment. The general condition of the rats, including body size, breathing rate, food intake, and voluntary physical activity, was evaluated daily. The survival status of all rats was observed from week 3 to week 10 after MCT injection.

CBS DEVICE IMPLANTATION. The CBS device was custom designed by Three-Lion Technologies. It is composed of a battery-powered impulse generator and a bipolar platinum electrode with conductive leads. The method of the electrode tip placement was described previously.[22] Briefly, a bipolar platinum electrode was implanted circumferentially around the right common carotid artery adjacent to the carotid sinus. The pulse generator was placed on the back subcutaneously. The threshold voltage was set at the level that could lead to a reduction in systolic blood pressure by 10%. The working voltage was set at 80% of the threshold voltage, with the stimulus frequency 10 Hz, pulse duration 1 ms, and a duty cycle of 5 minutes on and 1 minute off. The CBS model without any stimulus delivery was implanted in rats using the same method.

ECHOCARDIOGRAPHIC MEASUREMENT. Pulmonary acceleration time, RV ejection time, tricuspid annular plane systolic excursion, RV fractional area change, RV dimension in diastole, RV wall thickness, and cardiac output were measured.

NONINVASIVE BLOOD PRESSURE MEASUREMENT AND HEART RATE VARIABILITY ANALYSIS. Blood pressure was recorded using noninvasive pressure monitor on the tail artery. A 5-minute electrocardiographic recording was used for the analysis of total power, high frequency (HF) power spectrum, and low frequency (LF) power spectrum. The LF/HF ratio was also calculated.

FIGURE 1 Study Protocol

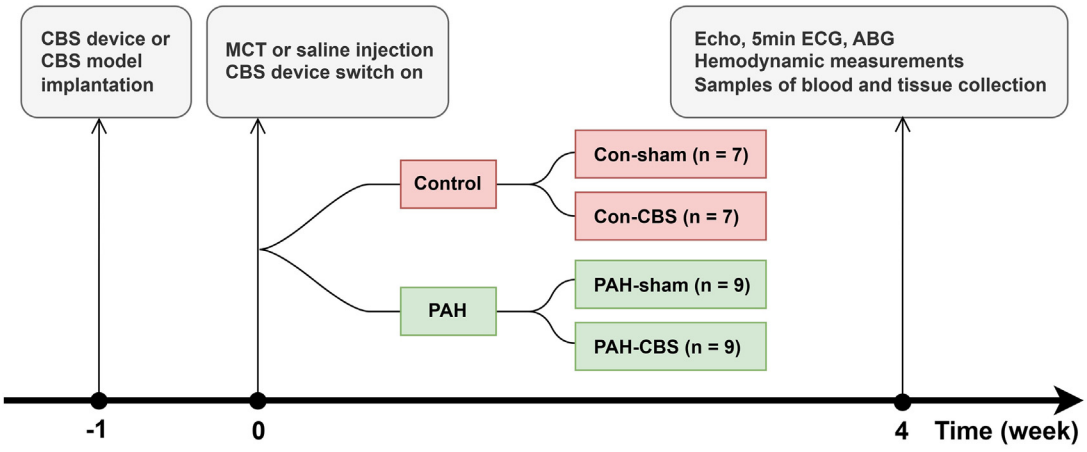

Con-sham group, n = 7; con–carotid baroreceptor stimulation (CBS) group, n = 7; pulmonary arterial hypertension (PAH)–sham group, n = 9; PAH-CBS group, n = 9. At week −1, the CBS device or CBS model was implanted; at week 0, a single intraperitoneal injection of monocrotaline (MCT) 60 mg/kg or saline was administered, and the CBS device was switched on. Four weeks after MCT injection, echocardiography (Echo), electrocardiography (ECG), arterial blood gas (ABG) analysis, and hemodynamic measurements were performed, and samples of blood and tissue were collected.

HEMODYNAMIC EVALUATION. Measurement of mean PAP. A homemade PE-50 catheter filled with heparin was connected to a pressure transducer. Then, the catheter was inserted into main PA through right external jugular vein to detect PAP. Mean PAP was analyzed using LabChart Pro 7.0 (ADInstruments). Pulmonary vascular resistance was calculated as mean PAP/cardiac output.

RV pressure-volume loop. The RV was punctured with a 24-gauge remaining needle. A combined pressure-volume Millar catheter was inserted into the RV and positioned. RV systolic pressure was acquired automatically from steady-state measurements, as well as arterial elastance (Ea) for the assessment of RV afterload. During the vena cava occlusion, end-systolic elastance (Ees) (a measure of RV contractility) and end-diastolic elastance (Eed) (a measure of RV filling) were determined. Also, the Ees/Ea ratio was calculated to evaluate RV-arterial coupling.

ARTERIAL BLOOD GAS AND HEPATORENAL FUNCTION. Arterial blood samples were taken from abdominal aorta to measure arterial Pa_{O2}, arterial Pa_{CO2}, arterial oxygen saturation, pH, and HCO_3^-. Vein blood samples were obtained from the inferior vena cava to detect the levels of alanine transaminase, aspartate aminotransferase, creatinine, and blood urea nitrogen.

HISTOLOGY. The weight ratio of RV to body weight, the weight ratio of RV to the left ventricle plus septum, and RV cardiomyocyte cross-sectional area, were calculated to evaluate RV hypertrophy. Cross-sectional area was evaluated using hematoxylin and eosin staining. RV tissue sections were analyzed using Masson trichrome staining and the collagen volume fraction was calculated to evaluate RV fibrosis. Lung paraffin sections were stained with hematoxylin and eosin for wall thickness percentage analysis.

IMMUNOHISTOCHEMISTRY AND IMMUNOFLUORESCENCE. The lung sections were stained with proliferating cell nuclear antigen and terminal deoxynucleotidyl transferase-mediated nick-end labeling to evaluate the proliferation and apoptosis of PA smooth muscle cells in pulmonary arterioles, respectively. Immunofluorescence double staining for α-smooth muscle actin and von Willebrand factor was performed to assess the expression of von Willebrand factor in endothelial cells and the muscularization of pulmonary arterioles. Immunohistochemical staining for tyrosine hydroxylase (TH) was used to assess the sympathetic nerve around the PA trunk and bifurcations.

WESTERN BLOTTING. Western blotting for matrix metallopeptidase-2 and -9 was performed in RV tissue.

QUANTITATIVE REAL-TIME REVERSE TRANSCRIPTION POLYMERASE CHAIN REACTION ANALYSIS. Expression of messenger RNA for atrial natriuretic peptide and B-type natriuretic peptide was measured in RV tissue.

TRANSCRIPTOME ANALYSIS. For RNA sequencing analysis, intralobar artery explants were excised quickly and snap frozen at −80 °C for the further analysis.

Additional details are presented in the Supplemental Methods.

STATISTICAL ANALYSIS. All data are presented as mean ± SEM. The Shapiro-Wilk normality test was used to evaluate data distribution. For normally distributed data, differences among the 4 groups were analyzed using 1-way analysis of variance. If Levene's test was not significant ($P > 0.05$), Tukey's post hoc test for multiple pairwise comparisons was used; otherwise, Tamhane's T2 post hoc test was used ($P \leq 0.05$). For non-normally distributed data, differences among the 4 groups were analyzed using the nonparametric Kruskal-Wallis test, and Dunn's post hoc test was performed for multiple pairwise comparisons. Survival was estimated using the Kaplan-Meier method and compared using the log-rank test. A P value <0.05 was considered to indicate statistical significance. SPSS version 23.0 (IBM) and R version 4.2.2 (R Foundation for Statistical Computing) were used for statistical analysis.

RESULTS

EFFECT OF CBS ON SURVIVAL RATE IN MCT-INDUCED PAH RATS. In the survival study, the rats with MCT injection exhibited evident clinical manifestations of PAH, including tachypnea, poor appetite, weight loss, and reduced physical activity. Correspondingly, death occurred over time. However, CBS treatment significantly prolonged survival time and improved the survival rate of MCT-induced PAH rats ($P = 0.046$, log-rank test) (Figure 2).

In the pathophysiological study, 1 rat in the PAH-sham group died 26 days after MCT injection, and in some rats it was not possible to obtain ideal echocardiographic images or perform measurements of pulmonary hemodynamic status, collect arterial or venous blood samples, or isolate intralobar artery explants. As a result, data for certain pathophysiological indicators were absent for some rats. Additionally, because of limited availability of RV tissue, a portion was used for western blotting detection while another portion was allocated for quantitative real-time reverse transcription polymerase chain reaction analysis. All successfully obtained data for each indicator were used for statistical analysis and are presented in the figures and table; specific n values are also indicated in the legends.

FIGURE 2 Effect of CBS on Survival Rate in Rats With MCT-Induced PAH

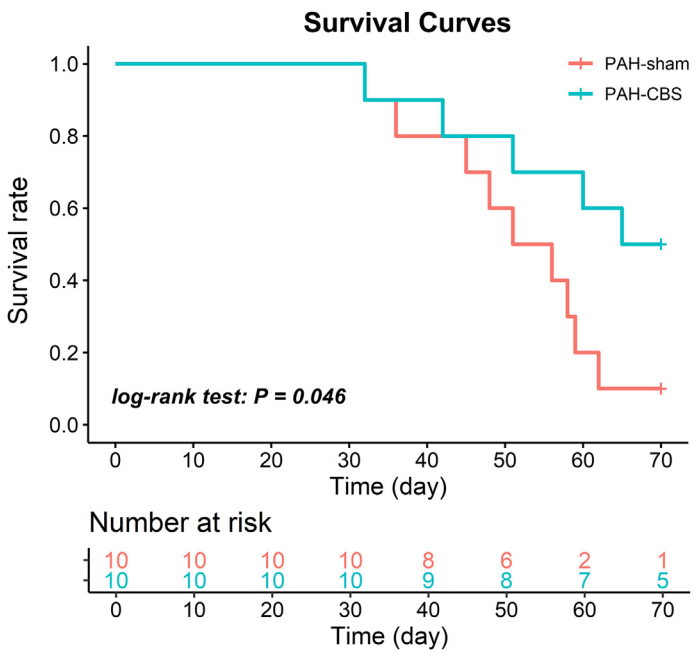

CBS markedly improved survival rate in rats with MCT-induced PAH ($P = 0.046$, log-rank test). PAH-sham group, n = 10; PAH-CBS group, n = 10. Survival was estimated using the Kaplan-Meier method. Abbreviations as in Figure 1.

EFFECTS OF CBS ON ARTERIAL BLOOD GAS AND HEPATORENAL FUNCTION IN MCT-INDUCED PAH RATS. Four weeks after MCT injection, systolic blood pressure and diastolic blood pressure in the PAH-sham group were significantly decreased compared with the con-sham group, with no significant change in heart rate. Pa_{O2}, Pa_{CO2}, arterial oxygen saturation, and HCO_3^- were significantly lower in the PAH-sham group compared with the con-sham group, with no significant change in pH value. In contrast, CBS treatment significantly reversed the decreases in systolic blood pressure, diastolic blood pressure, Pa_{O2}, and arterial oxygen saturation in PAH rats. Rats with PAH had higher levels of aspartate aminotransferase, creatinine, and blood urea nitrogen compared with control animals. CBS significantly inhibited the increase of blood urea nitrogen, without an influence on aspartate aminotransferase and creatinine, in PAH rats. There were no significant differences in the parameters of arterial blood gas and hepatorenal function in rats between the con-sham and con-CBS groups (Table 1).

JACC: BASIC TO TRANSLATIONAL SCIENCE VOL. 9, NO. 4, 2024
APRIL 2024:475–492

TABLE 1 Effects of CBS on Arterial Blood Gas and Hepatorenal Function in Monocrotaline-Induced PAH Rats

	Con-Sham	Con-CBS	PAH-Sham	PAH-CBS
Pao_2, mm Hg	93.00 ± 4.56	103.40 ± 5.06	61.80 ± 5.02[a]	83.00 ± 5.14[b,c]
$Paco_2$, mm Hg	45.00 ± 2.27	44.20 ± 1.16	33.30 ± 1.16[d]	37.25 ± 5.43
Sao_2, %	97.25 ± 0.48	98.00 ± 0.32	91.00 ± 1.87[a]	96.00 ± 0.71[b]
pH	7.43 ± 0.02	7.42 ± 0.00	7.45 ± 0.02	7.40 ± 0.02
HCO_3^-, mmol/L	29.78 ± 0.72	28.40 ± 0.71	23.12 ± 1.03[a]	22.95 ± 2.32
ALT, U/L	54.25 ± 3.94	43.20 ± 1.95	48.25 ± 4.18	49.75 ± 5.35
AST, U/L	109.00 ± 12.28	108.40 ± 11.99	163.25 ± 15.12[d]	138.30 ± 20.57
BUN, mmol/L	5.66 ± 0.18	5.96 ± 0.64	10.20 ± 0.47[e]	8.24 ± 0.70[b,f]
Cr, μmol/L	25.00 ± 0.70	27.40 ± 1.20	32.00 ± 1.78[d]	35.25 ± 1.24[f]
SBP, mm Hg	137.46 ± 6.57	139.34 ± 5.25	105.40 ± 5.84[a]	121.80 ± 4.92[b,c]
DBP, mm Hg	98.74 ± 3.09	112.58 ± 4.40	82.13 ± 3.97[a]	93.81 ± 2.52[b,f]
HR, beats/min	410.73 ± 8.91	418.47 ± 14.85	372.75 ± 9.70	374.74 ± 18.03[c]

Values are mean ± SEM. CBS significantly reversed the decreases in Pao_2, Sao_2, SBP, and DBP in PAH rats and inhibited the increase of BUN, without an influence on AST and Cr. Analysis of arterial blood gas and hepatorenal function: n = 4 or 5 for each group; noninvasive blood pressure measurement: n = 5 to 8 for each group; HR: n = 6 to 9 for each group. [a]$P < 0.01$ vs con-sham. [b]$P < 0.05$ vs PAH-sham. [c]$P < 0.05$ vs con-CBS. [d]$P < 0.05$ vs con-sham. [e]$P < 0.001$ vs con-sham. [f]$P < 0.01$ vs con-CBS by 1-way analysis of variance followed by Tukey or Tamhane T2 post hoc test or Kruskal-Wallis test followed by Dunn post hoc test.

ALT = alanine transaminase; AST = aspartate aminotransferase; BUN = blood urea nitrogen; CBS = carotid baroreceptor stimulation; Cr = creatinine; HCO_3^- = bicarbonate ion; DBP = diastolic blood pressure; HR = heart rate; PAH = pulmonary arterial hypertension; Sao_2 = blood oxygen saturation; SBP = systolic blood pressure.

EFFECTS OF CBS ON PAP AND RV PRESSURE-VOLUME LOOP IN MCT-INDUCED PAH RATS. Hemodynamic results showed that severe PAH occurred in the PAH-sham group 4 weeks after MCT injection, as reflected by significant increases in mean PAP, pulmonary vascular resistance, and RV systolic pressure (Figures 3B to 3D), obvious RV dilation (Figure 3E), and a marked reduction in RV ejection fraction (Figure 3F) compared with those in the con-sham group. However, treatment with CBS partly amended the hemodynamic disturbances (Figures 3B to 3D) (mean PAP 29.20 ± 3.17 mm Hg vs 46.22 ± 3.33 mm Hg [$P = 0.001$]; mean pulmonary vascular resistance 1.19 ± 0.43 mm Hg/L · min vs 2.49 ± 0.51 mm Hg/L · min [$P = 0.17$]; mean RV systolic pressure 56.22 ± 2.67 mm Hg vs 80.96 ± 4.58 mm Hg [$P < 0.001$]), ameliorated RV dilatation, and improved RV systolic function (Figures 3E and 3F) in PAH rats.

A representative example of an RV pressure-volume loop is shown in Figure 3A. MCT resulted in a significant increase in RV afterload (Ea) and RV filling (Eed) in rats in the PAH-sham group, whereas augmented RV contractility (Ees) was not commensurate with changes in RV afterload, leading to RV-arterial uncoupling (Ees/Ea) (Figures 3G to 3J). CBS treatment reduced RV afterload (Figure 3I) (mean Ea 0.58 ± 0.03 mm Hg/μL vs 0.93 ± 0.07 mm Hg/μL; $P = 0.021$) and RV diastolic stiffness (Figure 3H) (mean Eed 0.016 ± 0.002 mm Hg/μL vs 0.031 ± 0.004 mm Hg/μL; $P = 0.042$), improved RV contractility (Figure 3G) (mean Ees 0.67 ± 0.09 mm Hg/μL vs 0.45 ± 0.02 mm Hg/μL; $P = 0.008$), and partially normalized the RV-arterial uncoupling (Figure 3J) (mean Ees/Ea ratio 1.15 ± 0.13 vs 0.50 ± 0.05; $P = 0.005$) in PAH rats.

EFFECTS OF CBS ON PULMONARY FLOW AND RV FUNCTION IN MCT-INDUCED PAH RATS. As depicted in Figure 4A, pulmonary flow was altered in PAH rats, with faster pulmonary acceleration time and a marked decrease in pulmonary acceleration time/ejection time ratio, in line with mean PAP (Figures 3B and 3D). However, CBS partly normalized the changes in pulmonary acceleration time and pulmonary acceleration time/ejection time (Figures 4C and 4D) (mean pulmonary acceleration time 36.20 ± 2.92 ms vs 16.00 ± 0.65 ms vs 20.44 ± 0.87 ms; mean pulmonary acceleration time/ejection time ratio 41.24% ± 3.02% vs 17.46% ± 0.95% vs 23.55% ± 1.15%) in rats with PAH. As shown in Figure 4B, RV was dramatically dilated, and the interventricular septum was straight in PAH rats. The aforementioned morphologic abnormalities were alleviated after 4-week CBS treatment. Next, RV wall thickness and RV dimension in diastole were measured to further evaluate RV morphology. It was shown that RV wall thickness and RV dimension in diastole increased significantly, while CBS caused a marked decrease in RV wall thickness (Figure 4E) and RV dimension in diastole (Figure 4F) in PAH rats, indicating that CBS could partially restore the structural abnormality of the RV. Additionally, tricuspid annular plane systolic excursion and RV fractional area change were measured to assess RV systolic function. Tricuspid annular plane systolic excursion and RV fractional area change were higher in the PAH-CBS group than in the PAH-sham group (Figures 4G and 4H) (mean tricuspid annular plane systolic excursion 2.69 ± 0.16 mm vs 2.09 ± 0.19 mm [$P = 0.021$]; mean RV fractional area change 37.12% ± 2.53% vs 19.69% ± 1.67% [$P < 0.001$]), demonstrating that CBS could improve RV systolic function in rats with PAH. No significant differences were observed in echocardiographic measurements between the con-sham group and the con-CBS group (Figures 4A to 4H).

EFFECTS OF CBS ON PULMONARY ARTERIAL REMODELING IN MCT-INDUCED PAH RATS. As shown in Figures 5A to 5D, compared with con-sham rats, PAH-sham rats had significantly increased wall thickness percentage (diameter between 20 and 50 μm: 66.56% ± 3.02% vs 30.57% ± 2.22% [$P < 0.001$]; diameter between 50 and 150 μm: 56.57% ± 3.75% vs 28.41% ± 2.26% [$P < 0.001$]), increased expression of von Willebrand factor in endothelial cells of

FIGURE 3 **Effects of CBS on Pulmonary Arterial Pressure and RV Pressure-Volume Loop in MCT-Induced PAH Rats**

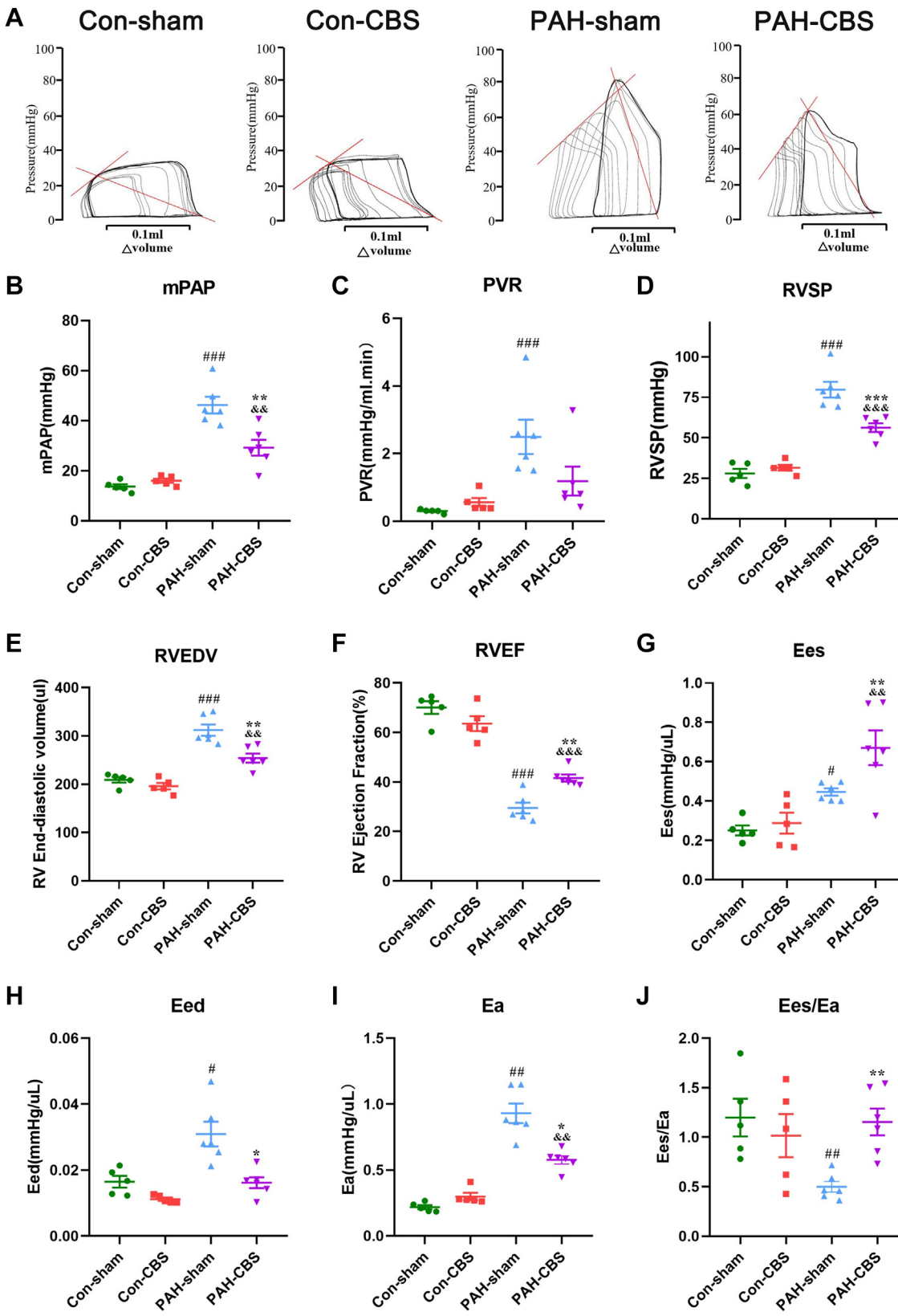

Continued on the next page

pulmonary arterioles, and increased muscularization degree of pulmonary arterioles, suggesting the deteriorative pulmonary arterial remodeling. In detail, the rate of nonmuscularized and partially muscularized pulmonary arterioles was decreased, whereas the rate of fully muscularized pulmonary arterioles was increased sharply in PAH rats compared with control animals (Figure 5J). In contrast, CBS partially improved pulmonary arterial remodeling in PAH-CBS rats compared with PAH-sham rats, as reflected by a significant decrease in wall thickness percentage (Figures 5G and 5H) (56.02% ± 3.13% vs 66.56% ± 3.02% [$P = 0.014$]; 43.68% ± 2.81% vs 56.57% ± 3.75% [$P = 0.004$]), reduced von Willebrand factor expression in endothelial cells (Figure 5I), and a reduction in the rate of fully muscularized pulmonary arterioles (Figure 5J). Also, the rate of nonmuscularized and partially muscularized pulmonary arterioles was significantly increased in PAH-CBS rats compared with PAH-sham rats (Figure 5J).

As shown in Figure 5E, the PAH rats had a higher percentage of proliferating cell nuclear antigen-positive PA smooth muscle cells compared with control animals (Figure 5K) (31.42% ± 2.18% vs 1.62% ± 0.47%; $P < 0.001$), with commensurate changes in wall thickness percentage. Excitingly, the percentage of proliferating cell nuclear antigen-positive PA smooth muscle cells in pulmonary arterioles was considerably reduced in PAH rats treated with CBS compared with PAH-sham rats (Figure 5K) (18.99% ± 3.06% vs 31.42% ± 2.18%; $P = 0.042$). The PA smooth muscle cell apoptosis index of pulmonary arterioles showed no difference in PAH rats with or without CBS treatment compared with normal control animals (Figures 5F and 5L). In addition, there were no significant difference in wall thickness percentage, the muscularization of distal pulmonary arterioles, and the proliferation and apoptosis of PA smooth muscle cells between the con-sham group and the con-CBS group (Figures 5A to 5L).

EFFECTS OF CBS ON RV REMODELING IN RATS WITH MCT-INDUCED PAH. Representative photomicrographs of RV tissue hematoxylin and eosin staining are shown in Figure 6A. It was found that the cardiac-pulmonary weight, the ratio of RV to body weight, the ratio of RV to left ventricle plus septum, and the cross-sectional area of RV cardiomyocytes were all increased significantly in PAH rats compared with normal control animals (Figures 6C to 6F). Moreover, the messenger RNA expression of atrial natriuretic peptide and B-type natriuretic peptide was up-regulated in the PAH rats (Figures 6K and 6L). However, with the exception of cardiac-pulmonary weight and messenger RNA expression of B-type natriuretic peptide, the other aforementioned parameters were partially reversed by CBS treatment (Figures 6C to 6F, 6K, and 6L), suggesting that CBS could alleviate RV hypertrophy in PAH rats.

Representative photomicrographs of RV tissue Masson trichrome staining are shown in Figure 6B. The collagen volume fraction and the protein expression of fibrotic markers (matrix metallopeptidase 2 and matrix metallopeptidase 9) in RV tissue were higher in PAH rats than that in normal control animals (Figures 6G to 6J). Conversely, CBS dramatically reduced the collagen volume fraction and the protein expression levels of matrix metallopeptidase 2 and matrix metallopeptidase 9 in PAH rats (Figures 6G to 6J). However, no significant differences in the aforementioned parameters associated with RV hypertrophy and fibrosis were observed between the con-sham group and the con-CBS group (Figures 6A to 6L).

EFFECTS OF CBS ON HEART RATE VARIABILITY POWER SPECTRAL ANALYSIS AND PA SYMPATHETIC INNERVATION IN MCT-INDUCED PAH RATS. Short-term power spectral analysis of heart rate variability showed the PAH-sham rats had significant reduction in total power, LF power, and HF power and a marked increase

FIGURE 3 Continued

Representative examples of right ventricular (RV) pressure-volume loop at the fourth week after MCT injection (A). After preload reduction (temporary inferior vena cava occlusion), multiple end-systolic pressure and volume points were performed, and the RV end-systolic pressure-volume relationship was identified (solid rising red line in A). Its slope was a load-independent measurement of RV contractility (end-systolic elastance [Ees]). The RV end-diastolic pressure-volume relationship and RV stiffness (end-diastolic elastance [Eed]) were obtained after preload reduction. RV afterload (arterial elastance [Ea]) was measured by RV end-systolic pressure in a steady state divided by stroke volume (descending solid red line in A). CBS decreased mean pulmonary artery pressure (mPAP) (B) and RV systolic pressure (RVSP) (D) in PAH rats. CBS reduced RV end-diastolic volume (RVEDV) (E) and increased RV ejection fraction (RVEF) (F) in PAH rats. CBS significantly decreased RV afterload (Ea) (I), improved RV contractility (Ees) (G), and reduced RV stiffness (Eed) (H), resulting in partial normalization of RV-arterial uncoupling (Ees/Ea) (J) in PAH rats. Con-sham group, n = 5; con-CBS group, n = 5; PAH-sham group, n = 6; PAH-CBS group, n = 6. Values are mean ± SEM. #$P < 0.05$ vs con-sham, ##$P < 0.01$ vs con-sham, and ###$P < 0.001$ vs con-sham; *$P < 0.05$ vs PAH-sham, **$P < 0.01$ vs PAH-sham, and ***$P < 0.001$ vs PAH-sham; &$P < 0.05$ vs. con-CBS, &&$P < 0.01$ vs con-CBS, and &&&$P < 0.001$ vs con-CBS by 1-way analysis of variance followed by Tukey or Tamhane T2 post hoc test or Kruskal-Wallis test followed by Dunn post hoc test. PVR = pulmonary vascular resistance; other abbreviations as in Figure 1.

FIGURE 4 **Effects of CBS on Pulmonary Flow and RV Function in MCT-Induced PAH Rats**

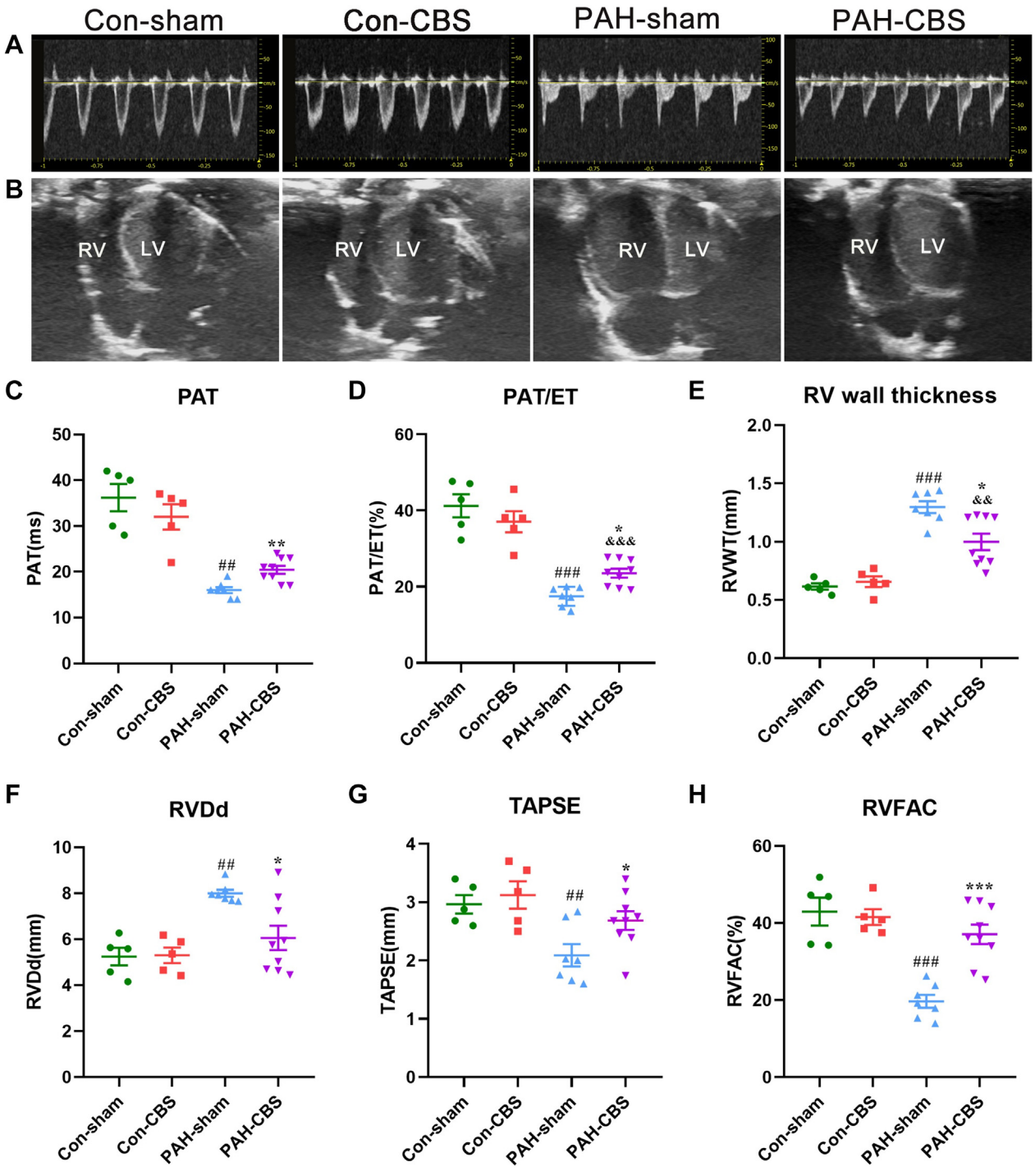

Representative images of pulmonary blood flow (A) and apical 4-chamber view (B) at the fourth week after MCT injection. CBS increased pulmonary acceleration time (PAT) (C) and PAT/ejection time (ET) ratio (D) in PAH rats. CBS decreased RV wall thickness (RVWT) (E) and RV dimension in diastole (RVDd) (F) in PAH rats. CBS increased tricuspid annular plane systolic excursion (TAPSE) (G) and RV fractional area change (RVFAC) (H) in PAH rats. Con-sham group, n = 5; con-CBS group, n = 5; PAH-sham group, n = 7; PAH-CBS group, n = 9. Values are mean ± SEM. ##$P < 0.01$ vs con-sham and ###$P < 0.001$ vs con-sham; *$P < 0.05$ vs PAH-sham, **$P < 0.01$ vs PAH-sham, and ***$P < 0.001$ vs PAH-sham; &&$P < 0.01$ vs con-CBS and &&&$P < 0.001$ vs con-CBS by 1-way analysis of variance followed by Tukey or Tamhane T2 post hoc test. LV = left ventricle; other abbreviations as in Figures 1 and 3.

FIGURE 5 Effects of CBS on Pulmonary Arterial Remodeling in Rats With Monocrotaline-Induced PAH

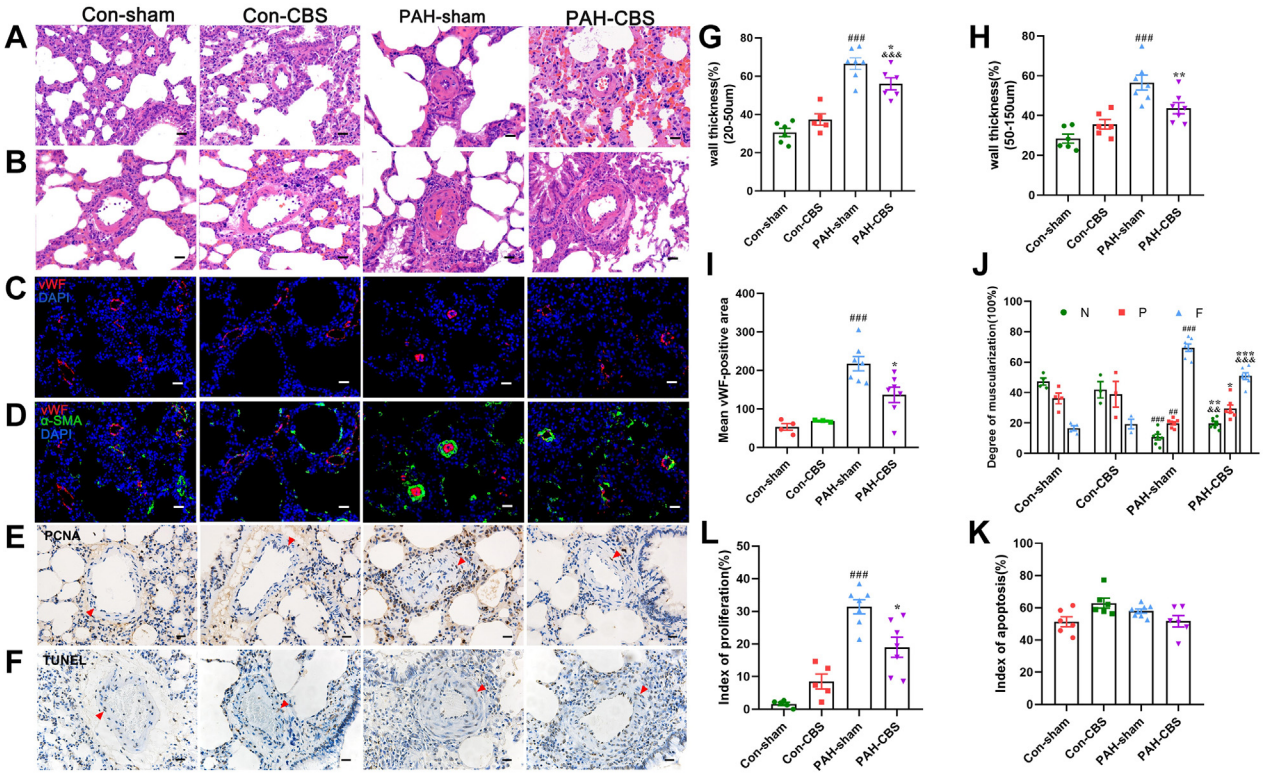

Representative photomicrographs of pulmonary arterioles with hematoxylin and eosin stain (A, diameter between 20 and 50 μm; B, diameter between 50 and 150 μm), with immunofluorescence staining for von Willebrand factor (vWF) (red), alpha smooth muscle actin (a-SMA) (green), and nuclei (4′,6-diamidino-2-phenylindole [DAPI]) (C, D) and with proliferating cell nuclear antigen (PCNA) immunohistochemical staining (E) and terminal deoxynucleotidyl transferase–mediated nick-end labeling (TUNEL) staining (F). CBS caused a marked reduction in the wall thickness percentage (G, H), expression of vWF in endothelial cells (I), and muscularization degree of pulmonary arterioles (J) in PAH rats. CBS partially reversed the increase in the percentage of PCNA-positive pulmonary artery smooth muscle cells (PASMCs) of pulmonary arterioles in PAH rats (K). The PASMC apoptosis index of pulmonary arterioles showed no difference in PAH rats with or without CBS treatment compared with normal control animals (L). No significant differences were observed in the aforementioned parameters between con-sham and con-CBS rats (A to L). The red arrows represent PCNA-positive nuclei (E) and TUNEL-positive nuclei (F). Scale bar, 20 μm (A to F). In G, H, and K, n = 5 to 7 for each group; in I and J, n = 3 to 7 for each group; in L, n = 6 to 8 for each group. Values are mean ± SEM. ##$P < 0.01$ vs con-sham and ###$P < 0.001$ vs con-sham; *$P < 0.05$ vs PAH-sham, **$P < 0.01$ vs PAH-sham, and ***$P < 0.001$ vs PAH-sham; &&$P < 0.01$ vs con-CBS and &&&$P < 0.001$ vs con-CBS by 1-way analysis of variance followed by Tukey or Tamhane T2 post hoc test. F = full muscularization; N = no muscularization; P = partial muscularization; other abbreviations as in Figure 1.

in the LF/HF ratio compared with normal control animals. However, the decreases in total power and HF power and the increase in the LF/HF ratio observed in the PAH-sham rats were partially reversed by CBS treatment (Figure 7C). Additionally, CBS did not cause any significant change in short-term power spectrum of heart rate variability in the rats without PAH (Figure 7C).

As shown in Figures 7A and 7B, TH-positive nerve fibers innervated in the connective and adipose tissue around the PA trunk and bifurcations. TH-positive innervation was significantly increased in PAH rats and was partially reversed after a 4-week CBS treatment. TH-positive innervation in rats in the con-CBS group was similar to that in the con-sham group. Additionally, the quantification of TH-positive innervation, expressed as the area of TH-positive nerves, revealed a significant reduction in TH-positive innervation around the PA trunk and bifurcations after CBS treatment in PAH-CBS rats compared with PAH-sham rats (Figure 7E) (12,475.18 ± 1,591.59 μm^2 vs 20,168.93 ± 2,494.94 μm^2; $P = 0.006$).

THE UNDERLYING MECHANISMS INVOLVED IN THE PROTECTIVE EFFECTS OF CBS AGAINST MCT-INDUCED PAH. At the end of the experiment, intralobar artery explants were excised for RNA sequencing analysis. As shown in the heat map

FIGURE 6 **Effects of CBS on RV Remodeling in Monocrotaline-Induced PAH Rats**

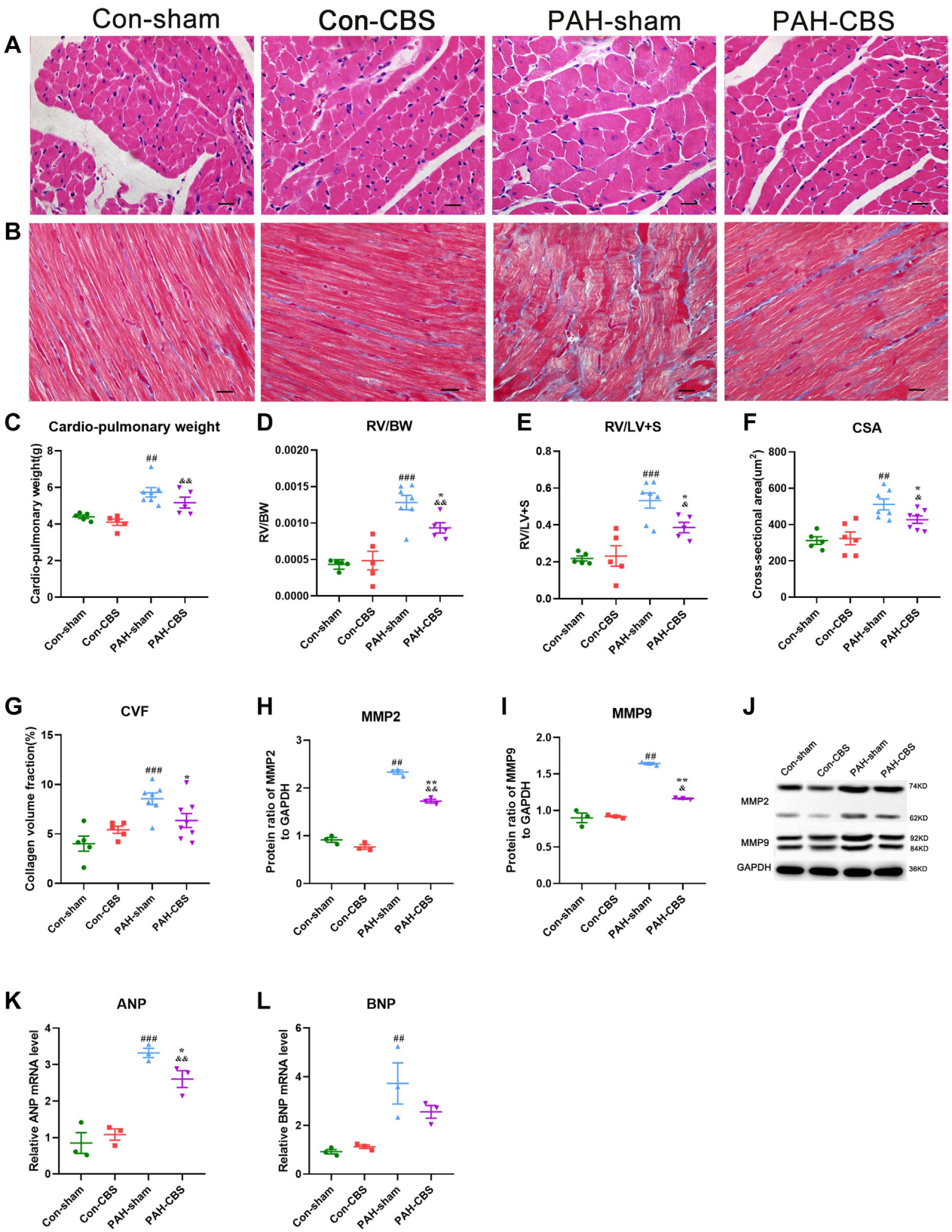

Continued on the next page

(**Figure 8A**), it was found that 1,722 genes were up-regulated and 1,218 genes were down-regulated in the PAH-sham group compared with the con-sham group (Supplemental Table 1). A total of 79 differential genes were amended by CBS intervention, with 32 down-regulated genes and 47 up-regulated genes (**Figures 8C and 8D**, Supplemental Tables 2 and 3). Gene Ontology enrichment revealed that these differential genes were involved in inflammatory immune responses, regulating the production of type I interferon, tumor necrosis factor, interleukin-6, interleukin-8, and activating α-β T cells. In addition, CBS also played a key role in the regulation of axonogenesis (**Figure 8E**). The protein-protein interaction network construction of these 79 differential genes indicated that the top 10 hub genes were closely related to inflammatory immune responses (**Figure 8F**).

DISCUSSION

The main findings of this study were as follows: 1) CBS improved the survival rate of rats with MCT-induced PAH; 2) CBS partially reversed the increases in mean PAP and RV systolic pressure, improved RV afterload (Ea), RV contractility (Ees), and filling (Eed), and normalized RV-arterial coupling (Ees/Ea) in PAH rats; 3) CBS caused an inhibition of pulmonary arterial remodeling and the proliferation of PA smooth muscle cells, improved RV performance, and delayed RV hypertrophy and fibrosis in PAH rats; and 4) CBS alleviated sympathovagal imbalance and decreased the sympathetic nerve density around the PA trunk and bifurcations in PAH rats. The results of RNA sequencing analysis indicated that the suppression of inflammatory immune responses might be the mechanisms by which CBS treatment alleviated pulmonary arterial remodeling in PAH rats.

CBS SUPPRESSED INFLAMMATION AND IMMUNE RESPONSES IN PAH RATS. Dysregulation of inflammation is a hallmark of PAH. Increased levels of serum proinflammatory markers have been reported in patients with various types of PAH, which are closely related to the prognosis and can be used for risk stratification of PAH.[24] Pulmonary vascular plexiform lesions are characterized by varying degrees of perivascular immune cell accumulation and intravascular infiltration.[25] Mean pulmonary perivascular inflammation score positively correlated with pulmonary vascular thickness and mean PAP.[25] Several animal experiments have shown that inflammatory cytokines play an important role in the initiation and development of PAH.[26-28] For example, interleukin-6 promoted pulmonary vascular remodeling via pro-proliferative and antiapoptotic mechanisms in lung-specific overexpressed interleukin-6 transgenic mice.[26] In contrast, interleukin-6-deficient reduced inflammatory cell recruitment and protected against hypoxia-induced PAH.[27] Tumor necrosis factor-α suppressed vascular bone morphogenetic protein signaling and promoted the proliferation of PA smooth muscle cells, but anti-tumor necrosis factor-α immunotherapy reversed the progression of PAH and restored normal bone morphogenetic protein/NOTCH signaling.[28]

In our present study, the inflammatory-related pathways and inflammation-associated key genes were activated in an MCT-induced PAH rat model. CBS amended 79 differential genes in PAH rats, which were involved in inflammation and immune responses, regulating the production of type I interferon, tumor necrosis factor, interleukin-6, interleukin-8, and activating α-β T cells. The top 10 hub genes were all closely related to inflammatory immune responses. Specifically, the hub gene toll-like receptor 7 was involved in almost all of the aforementioned inflammatory immune pathways. A recent bioinformatics analysis suggested that toll-like receptor 7 might serve as a circulating biomarker and a possible therapeutic target for idiopathic patients with PAH.[29] In addition, our study revealed that CBS also modulated the nerve development signaling pathways involved in the regulation of axonogenesis, resulting in a reduction of sympathetic density around the PA trunk and bifurcations in PAH rats.

FIGURE 6 Continued

Representative photomicrographs of RV cardiomyocyte cross-sectional area (CSA) (A; hematoxylin and eosin stain) and RV fibrosis (B; Masson staining). Representative immunoblots of RV fibrotic markers (J). CBS significantly reduced RV/body weight (BW) (D), RV/LV plus septum (LV+S) (E), and RV cardiomyocyte CSA (F) in PAH rats. CBS ameliorated RV fibrosis (G) and down-regulated the protein expression of matrix metallopeptidase 2 (MMP2) (H) and MMP9 (I) in PAH rats. CBS also decreased the messenger RNA (mRNA) expression of atrial natriuretic peptide (ANP) (K) in PAH rats. No significant differences in the parameters aforementioned were observed between the con-sham and con-CBS groups (A to L). Scale bar, 20 μm (A, B). In C to F, n = 5 to 7 for each group; in G, n = 5 to 8 for each group; in H to L, n = 3 for each group. Values are mean ± SEM. ##$P < 0.01$ vs con-sham and ###$P < 0.001$ vs con-sham; *$P < 0.05$ vs PAH-sham and **$P < 0.05$ vs PAH-sham; &$P < 0.05$ vs con-CBS and &&$P < 0.01$ vs con-CBS by 1-way analysis of variance followed by Tukey or Tamhane T2 post hoc test. BNP = B-type natriuretic peptide; CVF = collagen volume fraction; GAPDH = glyceraldehyde 3-phosphate dehydrogenase; other abbreviations as in **Figures 1, 3, and 4**.

FIGURE 7 **Effects of CBS on HRV Power Spectral Analysis and PA Sympathetic Tone in Monocrotaline-Induced PAH Rats**

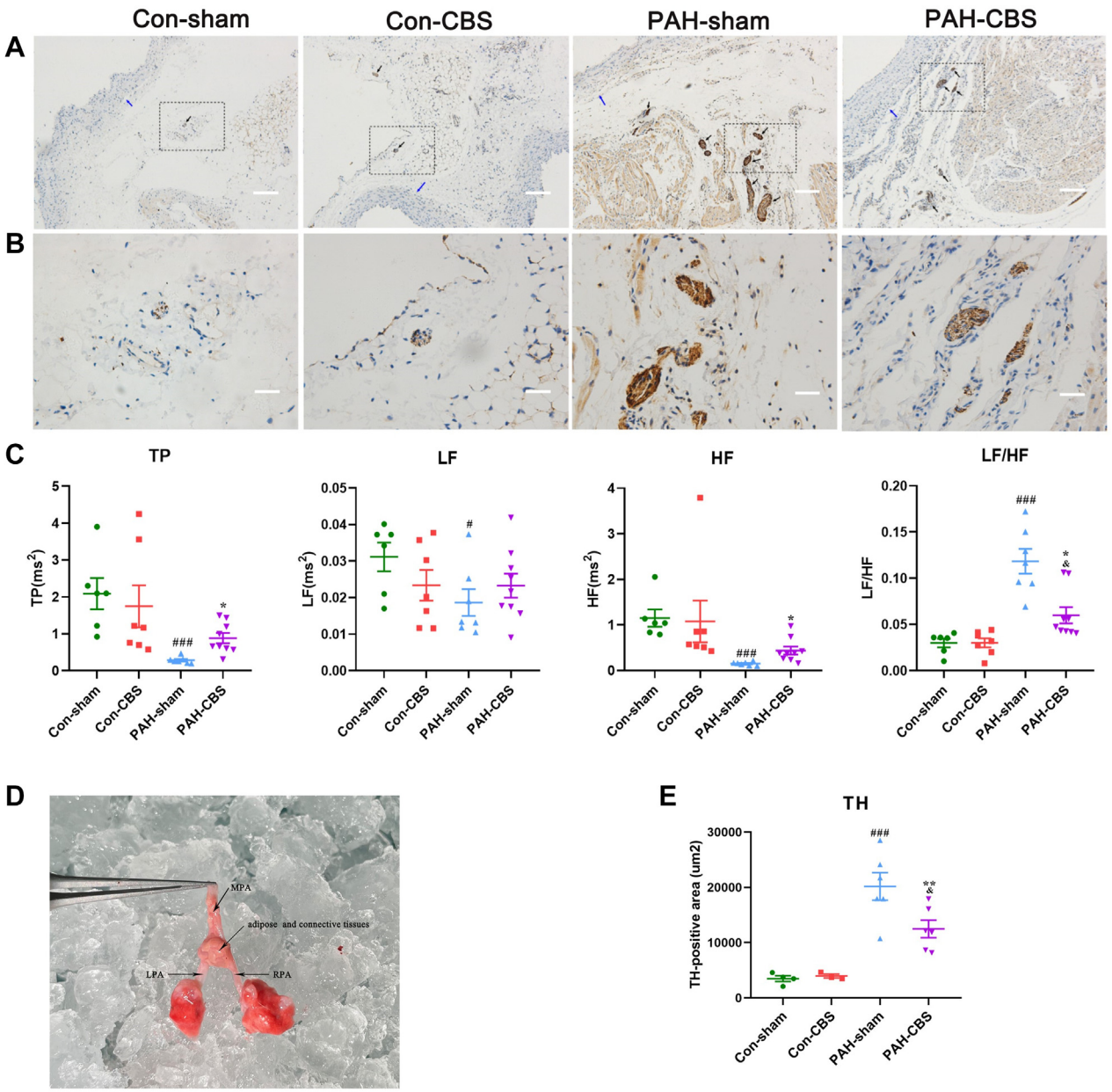

As shown by the representative immunohistochemistry photomicrographs, tyrosine hydroxylase (TH)-positive nerve bundles were localized mainly in adipose and connective tissue around the pulmonary artery (PA) trunk and adjacent right PA (RPA) and left PA (LPA) (A, B). The black arrow indicates the TH-positive nerve bundle, and the blue arrow indicates the PA (A). The bottom row image (B) is an enlarged version of the black dotted box in the top-row image (A). Scale bars,100 μm (A) and 20 μm (B). Representative anatomical image of the PA trunk and its bifurcations in rats (D). Short-term power spectral analysis of heart rate variability (HRV) showed that PAH rats had a significant reduction in total power (TP) and low-frequency (LF) and high-frequency (HF) power and an increase in LF/HF ratio compared with control animals, but the decreases of TP and HF power, as well as the increase in LF/HF ratio in PAH rats, were partially reversed by a 4-week CBS intervention (C). CBS reduced the area of TH-positive nerve bundles around the PA trunk and bifurcations in PAH rats (E). In C, n = 6 to 9 for each group; in E, n = 3 to 6 for each group. Values are mean ± SEM. #$P < 0.05$ vs con-sham, ##$P < 0.01$ vs con-sham, and ###$P < 0.001$ vs con-sham; *$P < 0.05$ vs PAH-sham and **$P < 0.01$ vs PAH-sham; &$P < 0.05$ vs con-CBS by 1-way analysis of variance followed by Tukey or Tamhane T2 post hoc test or Kruskal-Wallis test followed by Dunn post hoc test. MPA = main pulmonary artery; other abbreviations as in Figure 1.

JACC: BASIC TO TRANSLATIONAL SCIENCE VOL. 9, NO. 4, 2024
APRIL 2024:475–492

FIGURE 8 The Underlying Mechanisms Involved in the Protective Effects of CBS Against MCT-Induced PAH Rats

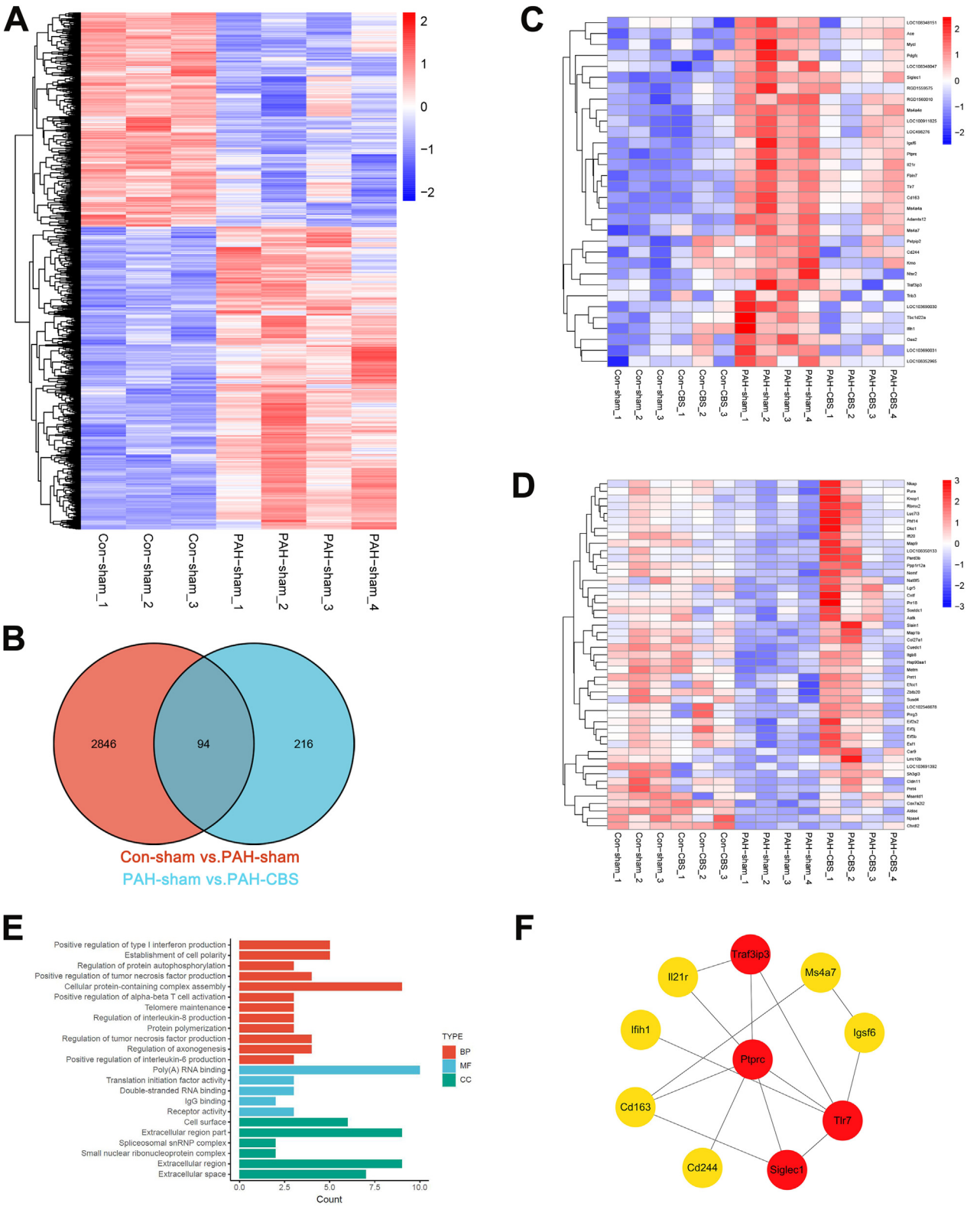

Continued on the next page

CBS INHIBITED SYMPATHETIC OVERACTIVATION IN PAH RATS. It has been demonstrated that patients with PAH had impaired heart rate variability,[30] blunted baroreflex sensitivity,[31] and lower HF component on spectral analysis,[5] which were associated with disease severity and prognosis. In agreement with others,[32,33] we found that total power and HF power were reduced after MCT injection, which indicated impaired heart rate variability and a decrease in parasympathetic activity tone, respectively. Interestingly, we found that LF power was decreased in the PAH rats, suggesting that chronic sympathetic activation led to a reduced responsiveness to changes in sympathetic tension. In addition, we found a significant increase in the LF/HF ratio in PAH rats, indicating sympathovagal imbalance. However, CBS alleviated autonomic nervous system imbalance in PAH, as evidenced by an increase in HF power and a decrease in the LF/HF ratio.

Similar to the arteries of other organs, the PA is innervated by abundant sympathetic fibers at its trunk and bifurcations.[6] Sympathetic overactivity was closely related to the prognosis and severity of PAH in patients.[30] Stimulation of pulmonary sympathetic nerve caused a frequency-dependent increase in pulmonary vascular resistance.[7] Moreover, smooth muscle cells of pulmonary precapillary increased sensitivity to catecholamines in hypoxia-induced PAH rats.[31] Excessive norepinephrine or neuropeptide Y released by the sympathetic nerve played a key role in the vasoconstriction of pulmonary vessels and proliferation of PA smooth muscle cells.[14,32] Both transection of the cervical sympathetic trunk[14] and PA denervation[17] caused marked improvements in hemodynamic status and pulmonary arterial remodeling in experimental models of PAH. PA denervation also reduced pulmonary vascular resistance, improved cardiac function, and increased 6-minute walk distance in patients with PAH.[18,19]

The crosstalk between the autonomic nervous system and the immune system exerted a powerful influence on the homeostasis of the cardiovascular system by modulating the release of neurohormones, inflammatory mediators, and chemokines.[34,35] The central autonomic nervous system can sense peripheral immune status through neural and non-neural communication pathways and maintains neural-immune communication mediated by neurotransmitters and neuromodulators.[36] Importantly, many types of immune cells express adrenergic and nicotinic receptors, which bind neurotransmitters to initiate immunomodulatory responses.[36,37] Meanwhile, cytokines and other immune mediators modulated the activity and responsivity of discharges in sympathetic and parasympathetic nerves innervating diverse targets.[36] Dysregulated inflammatory immune responses and neuroactive ligand-receptor signaling pathways were involved in the onset and development of PAH.[38] Donepezil, a cholinesterase inhibitor, effectively inhibited the differentiation and infiltration of inflammatory cells in lung tissue through cholinergic receptor pathway.[39]

In our present study, 4-week CBS intervention attenuated autonomic imbalance and reduced sympathetic innervation around the PA trunk and bifurcations in PAH rats, accompanied by the suppression of inflammatory immune responses. The inhibition of the sympathetic overactivation might be the potential mechanism involved in the suppression of inflammation by CBS treatment in MCT-induced PAH rats.

CBS IMPROVED PULMONARY ARTERIAL REMODELING AND RV DYSFUNCTION IN PAH RATS. The increased muscularization degree of pulmonary arterioles, the progressive arterial wall hypertrophy, and the proliferation of PA smooth muscle cells are the major features of pulmonary arterial remodeling in patients with PAH, which were associated with poor prognosis.[40] This plexogenic arteriopathy increases pulmonary vascular resistance and imposes a pressure overload on the RV, subsequently resulting in RV maladaptive remodeling and dysfunction. In our

FIGURE 8 Continued

(A) Heat map showing up-regulated or down-regulated differentially expressed genes (DEGs) in PAH rats induced with MCT. (B) Venn diagrams of DEGs between the con-sham and PAH-sham groups and the PAH-sham and PAH-CBS groups. (C) Cluster analysis of 32 down-regulated DEGs by CBS in PAH rats. (D) Cluster analysis of 47 up-regulated DEGs by CBS in PAH rats. (E) Functional classifications on the basis of Gene Ontology enrichment analysis of 79 genes with MCT-induced DGEs alterations regulated by CBS. (F) The top 10 hub genes of the protein-protein interaction network diagram of 79 differential genes with MCT-induced DEG alterations regulated by CBS; the more reddish and darker the color of the gene, the higher the protein-protein network score. n = 3 for the con-sham and con-CBS groups, n = 4 for the PAH-sham and PAH-CBS groups. BP = biological process; CC = cellular components; Cd163 = cluster of differentiation; Cd244, cluster of differentiation 244; Ifih1 = interferon induced with helicase C domain 1; Igsf6, immunoglobulin superfamily member 6; IL-21r, interleukin 21 receptor; MF = molecular function; Ms4a7 = membrane spanning 4-domains A7; PTPRC = protein tyrosine phosphatase, receptor type, C, CD45; Siglec1 = sialic acid binding Ig like lectin 1; TLR7 = toll-like receptor 7; Traf3ip3 = TRAF3 interacting protein 3; other abbreviations as in Figure 1.

present study, PAH rats showed subtotal occlusion of pulmonary arterioles, an increased degree of pulmonary arteriolar muscularization, and abnormal proliferation of PA smooth muscle cells. Remarkably, CBS significantly inhibited pulmonary arterial remodeling and the proliferation of PA smooth muscle cells in PAH rats.

Elevated RV afterload leads to RV dysfunction, which is one of the main prognostic determinants of PAH.[41] RV-arterial uncoupling mainly contributes to death in PAH.[42] To determine the effects of CBS on load-independent parameters of RV function, RV pressure volumes (the gold standard to evaluate RV function) were performed at the end of the present study. Our data showed that mean PAP was markedly attenuated after CBS intervention, which in turn led to reductions in RV afterload (Ea) and RV systolic pressure. As a result, RV hypertrophy and RV dysfunction were improved in PAH rats. A growing body of evidence[5,10,42] has shown that RV afterload (Ea) increases coupled with the disease severity of PAH, whereas Ees (RV contractility) cannot increase in parallel, leading to RV-arterial uncoupling (Ees/Ea). Interestingly, we found that CBS significantly reduced the increases in RV afterload (Ea) and RV diastolic stiffness (Eed) and improved RV contractility (Ees), resulting in a partial normalization of RV-arterial coupling (Ees/Ea) in MCT-induced PAH rats. The improvement of renal function by CBS in MCT-induced PAH rats might be attributed to the enhancement of RV and pulmonary hemodynamic status.

RV hypertrophy is an adaptive response to mechanical and hormonal stimuli, which eventually progresses into RV failure. Up-regulation of natriuretic peptides has been considered a hallmark of heart failure or myocardial hypertrophy. Levels of natriuretic peptides decrease with the improvement of cardiac function.[9] Sympathetic overactivation also triggered interstitial matrix remodeling and fibrosis by activating matrix metalloproteinases during the transition from hypertrophy to ventricular dilatation.[43] In the present study, CBS treatment improved cardiac hypertrophy in MCT-induced PAH rats, as evidenced by the reduction of RV wall thickness, RV/body weight ratio, RV/left ventricle plus septum weight ratio, RV cardiomyocyte cross-sectional area, and gene expression of atrial natriuretic peptide. Additionally, our data suggest that CBS attenuated RV fibrosis and RV dilation in PAH rats.

The suppression of sympathetic overactivation and inflammatory immune responses might be involved in the potential mechanism by which CBS improved PA remodeling in MCT-induced PAH rats. The protective action of CBS on RV function and remodeling might be due to the improvements in pulmonary hemodynamic status and PA remodeling. Additionally, it could be speculated that CBS directly improves RV structure and function by alleviating autonomic nervous system imbalance in PAH rats.

STUDY LIMITATIONS. In our present study, we implemented CBS intervention at the onset of PAH, with the aim of mitigating PAH progression; however, we did not explore its impact on established PAH. Additionally, the PAH model exclusively focused on MCT-induced PAH. Future investigation should strive to: 1) ascertain whether CBS can impede the progression of established PAH; 2) validate the safety and long-term efficacy of CBS in a secondary PAH model, particularly in left heart disease–related PAH; and 3) substantiate the clinical implications of CBS in treating patients with PAH.

CONCLUSIONS

Our findings suggest that CBS suppressed sympathetic overactivation, mitigated inflammatory immune responses, inhibited pulmonary arterial remodeling, and ameliorated RV dysfunction, thereby improving the survival rate of MCT-induced PAH rats. Our findings contribute to a deeper understanding of the underlying mechanism of autonomic nervous system imbalance in the pathogenesis and progression of PAH. CBS might serve as a promising intervention for clinical therapy for PAH by autonomic neuromodulation.

ACKNOWLEDGMENT The authors are grateful for the valuable comments provided by Prof Zhi-Gang She (Department of Cardiology, Renmin Hospital of Wuhan University, and Institute of Model Animal of Wuhan University).

FUNDING SUPPORT AND AUTHOR DISCLOSURES

This work was supported by the National Natural Science Foundation of China (grants 81970438 and 81770507) and the Interdisciplinary Innovative Talents Foundation from Renmin Hospital of Wuhan University (grant JCRCGW-2022-001). The authors have reported that they have no relationships relevant to the contents of this paper to disclose.

ADDRESSES FOR CORRESPONDENCE: Dr Mingwei Bao, Department of Cardiology, Renmin Hospital of Wuhan University, 238 Jiefang Road, Wuhan, Hubei, China. E-mail: mbao@whu.edu.cn. OR Dr Junxia Zhang, Department of Endocrinology, Taikang Tongji (Wuhan) Hospital, 322 Sixin North Road, Wuhan, Hubei, China. E-mail: zhangjx023@163.com.

PERSPECTIVES

COMPETENCY IN MEDICAL KNOWLEDGE: Autonomic nervous system imbalance is intricately associated with the severity and prognosis of PAH, but its specific mechanism in PAH development remains unclear. CBS is an innovative intervention for autonomic neuromodulation that has undergone extensive investigation as a potential treatment option for refractory hypertension, chronic heart failure, and arrhythmias. We investigate, for the first time, the effects of CBS on MCT-induced PAH and elucidate its underlying mechanisms. CBS reduces sympathetic tone and inflammatory immune response of PAs and ameliorates pulmonary arterial remodeling and RV dysfunction, exerting protective effects on the progression of PAH.

TRANSLATIONAL OUTLOOK: The present study enhances understanding of the mechanisms underlying autonomic nervous system imbalance in the pathogenesis and progression of PAH, broadening therapeutic options for PAH. CBS appears to be a promising strategy for the clinical treatment of patients with PAH in addition to established medical treatment.

REFERENCES

1. Humbert M, Kovacs G, Hoeper MM, et al. 2022 ESC/ERS guidelines for the diagnosis and treatment of pulmonary hypertension. *Eur Respir J*. 2023;61(1):2200879.

2. Thenappan T, Ormiston ML, Ryan JJ, Archer SL. Pulmonary arterial hypertension: Pathogenesis and clinical management. *BMJ*. 2018;360:j5492.

3. Farber HW, Miller DP, Poms AD, et al. Five-year outcomes of patients enrolled in the REVEAL registry. *Chest*. 2015;148:1043–1054.

4. Velez-Roa S, Ciarka A, Najem B, Vachiery JL, Naeije R, van de Borne P. Increased sympathetic nerve activity in pulmonary artery hypertension. *Circulation*. 2004;110:1308–1312.

5. da Silva Gonçalves Bós D, Van Der Bruggen CEE, Kurakula K, et al. Contribution of impaired parasympathetic activity to right ventricular dysfunction and pulmonary vascular remodeling in pulmonary arterial hypertension. *Circulation*. 2018;137:910–924.

6. Townsley MI. Structure and composition of pulmonary arteries, capillaries, and veins. *Compr Physiol*. 2012;2:675–709.

7. Kadowitz PJ, Hyman AL. Effect of sympathetic nerve stimulation on pulmonary vascular resistance in the dog. *Circ Res*. 1973;32:221–227.

8. Vaillancourt M, Chia P, Sarji S, et al. Autonomic nervous system involvement in pulmonary arterial hypertension. *Respir Res*. 2017;18:201.

9. Bogaard HJ, Natarajan R, Mizuno S, et al. Adrenergic receptor blockade reverses right heart remodeling and dysfunction in pulmonary hypertensive rats. *Am J Respir Crit Care Med*. 2010;182:652–660.

10. de Man FS, Handoko ML, van Ballegoij JJ, et al. Bisoprolol delays progression towards right heart failure in experimental pulmonary hypertension. *Circ Heart Fail*. 2012;5:97–105.

11. Perros F, Ranchoux B, Izikki M, et al. Nebivolol for improving endothelial dysfunction, pulmonary vascular remodeling, and right heart function in pulmonary hypertension. *J Am Coll Cardiol*. 2015;65:668–680.

12. Provencher S, Herve P, Jais X, et al. Deleterious effects of β-blockers on exercise capacity and hemodynamics in patients with portopulmonary hypertension. *Gastroenterology*. 2006;130:120–126.

13. van Campen JSJA, de Boer K, van de Veerdonk MC, et al. Bisoprolol in idiopathic pulmonary arterial hypertension: an explorative study. *Eur Respir J*. 2016;48:787–796.

14. Zhao Y, Xiang R, Peng X, Dong Q, Li D, Yu G, et al. Transection of the cervical sympathetic trunk inhibits the progression of pulmonary arterial hypertension via ERK-1/2 signalling. *Respir Res*. 2019;20:121.

15. Yoshida K, Saku K, Kamada K, et al. Electrical vagal nerve stimulation ameliorates pulmonary vascular remodeling and improves survival in rats with severe pulmonary arterial hypertension. *J Am Coll Cardiol Basic Trans Science*. 2018;3:657–671.

16. da Silva Goncalves Bos D, Happe C, Schalij I, et al. Renal denervation reduces pulmonary vascular remodeling and right ventricular diastolic stiffness in experimental pulmonary hypertension. *J Am Coll Cardiol Basic Trans Science*. 2017;2:22–35.

17. Zhou L, Zhang J, Jiang XM, et al. Pulmonary artery denervation attenuates pulmonary arterial remodeling in dogs with pulmonary arterial hypertension induced by dehydrogenized monocrotaline. *J Am Coll Cardiol Intv*. 2015;8:2013–2023.

18. Romanov A, Cherniavskiy A, Novikova N, et al. Pulmonary artery denervation for patients with residual pulmonary hypertension after pulmonary endarterectomy. *J Am Coll Cardiol*. 2020;76:916–926.

19. Zhang H, Zhang J, Chen M, et al. Pulmonary artery denervation significantly increases 6-min walk distance for patients with combined pre- and post-capillary pulmonary hypertension associated with left heart failure: the PADN-5 study. *J Am Coll Cardiol Intv*. 2019;12:274–284.

20. Halbach M, Fritz T, Madershahian N, Pfister R, Reuter H. Baroreflex activation therapy in heart failure with reduced ejection fraction: available data and future perspective. *Curr Heart Fail Rep*. 2016;13:71–76.

21. Wallbach M, Lehnig L-Y, Schroer C, et al. Effects of baroreflex activation therapy on ambulatory blood pressure in patients with resistant hypertension. *Hypertension*. 2016;67:701–709.

22. Yu Q, Shu L, Wang L, et al. Effects of carotid baroreceptor stimulation on aortic remodeling in obese rats. *Nutr Metab Cardiovasc Dis*. 2021;31:1635–1644.

23. Wang J, Yu Q, Dai M, et al. Carotid baroreceptor stimulation improves cardiac performance and reverses ventricular remodelling in canines with pacing-induced heart failure. *Life Sci*. 2019;222:13–21.

24. Soon E, Holmes AM, Treacy CM, et al. Elevated levels of inflammatory cytokines predict survival in idiopathic and familial pulmonary arterial hypertension. *Circulation*. 2010;122:920–927.

25. Rabinovitch M, Guignabert C, Humbert M, Nicolls MR. Inflammation and immunity in the pathogenesis of pulmonary arterial hypertension. *Circ Res*. 2014;115:165–175.

26. Steiner MK, Syrkina OL, Kolliputi N, Mark EJ, Hales CA, Waxman AB. Interleukin-6 overexpression induces pulmonary hypertension. *Circ Res*. 2009;104:236–244.

27. Savale L, Tu L, Rideau D, et al. Impact of interleukin-6 on hypoxia-induced pulmonary hypertension and lung inflammation in mice. *Respir Res*. 2009;10:6.

28. Hurst LA, Dunmore BJ, Long L, et al. TNFalpha drives pulmonary arterial hypertension by suppressing the BMP type-II receptor and altering Notch signalling. *Nat Commun*. 2017;8:14079.

29. Zhao E, Xie H, Zhang Y. Identification of differentially expressed genes associated with

idiopathic pulmonary arterial hypertension by integrated bioinformatics approaches. *J Comput Biol*. 2021;28(1):79–88.

30. Minai OA, Gudavalli R, Mummadi S, Liu X, McCarthy K, Dweik RA. Heart rate recovery predicts clinical worsening in patients with pulmonary arterial hypertension. *Am J Respir Crit Care Med*. 2012;185:400–408.

31. Mar PL, Nwazue V, Black BK, et al. Valsalva maneuver in pulmonary arterial hypertension: susceptibility to syncope and autonomic dysfunction. *Chest*. 2016;149:1252–1260.

32. Na S, Kim OS, Ryoo S, et al. Cervical ganglion block attenuates the progression of pulmonary hypertension via nitric oxide and arginase pathways. *Hypertension*. 2014;63:309–315.

33. Wensel R, Jilek C, Dorr M, et al. Impaired cardiac autonomic control relates to disease severity in pulmonary hypertension. *Eur Respir J*. 2009;34:895–901.

34. O'Mahony C, van der Kleij H, Bienenstock J, Shanahan F, O'Mahony L. Loss of vagal anti-inflammatory effect: in vivo visualization and adoptive transfer. *Am J Physiol Regul Integr Comp Physiol*. 2009;297:R1118–R1126.

35. Harwani SC, Chapleau MW, Legge KL, Ballas ZK, Abboud FM. Neurohormonal modulation of the innate immune system is proinflammatory in the prehypertensive spontaneously hypertensive rat, a genetic model of essential hypertension. *Circ Res*. 2012;111:1190–1197.

36. Kenney MJ, Ganta CK. Autonomic nervous system and immune system interactions. *Compr Physiol*. 2014;4:1177–1200.

37. Udit S, Blake K, Chiu IM. Somatosensory and autonomic neuronal regulation of the immune response. *Nat Rev Neurosci*. 2022;23:157–171.

38. Xiao G, Wang T, Zhuang W, et al. RNA sequencing analysis of monocrotaline-induced PAH reveals dysregulated chemokine and neuroactive ligand receptor pathways. *Aging (Albany NY)*. 2020;12:4953–4969.

39. Guo Y, He Z, Chen Z, et al. Inhibition of Th17 cells by donepezil ameliorates experimental lung fibrosis and pulmonary hypertension. *Theranostics*. 2023;13:1826–1842.

40. Pullamsetti SS, Savai R, Seeger W, Goncharova EA. Translational advances in the field of pulmonary hypertension. From cancer biology to new pulmonary arterial hypertension therapeutics. Targeting cell growth and proliferation signaling hubs. *Am J Respir Crit Care Med*. 2017;195:425–437.

41. Ryan JJ, Archer SL. The right ventricle in pulmonary arterial hypertension: disorders of metabolism, angiogenesis and adrenergic signaling in right ventricular failure. *Circ Res*. 2014;115:176–188.

42. Sanz J, Garcia-Alvarez A, Fernandez-Friera L, et al. Right ventriculo-arterial coupling in pulmonary hypertension: a magnetic resonance study. *Heart*. 2012;98:238–243.

43. Seeland U, Selejan S, Engelhardt S, Muller P, Lohse MJ, Bohm M. Interstitial remodeling in beta1-adrenergic receptor transgenic mice. *Basic Res Cardiol*. 2007;102:183–193.

KEY WORDS carotid baroreceptor stimulation, pulmonary arterial hypertension, pulmonary arterial remodeling, right ventricular dysfunction, sympathetic nervous system

APPENDIX For a supplemental Methods section, tables, and references, please see the online version of this paper.